EPJ Web of Conferences **21**, 04004 (2012)
DOI: 10.1051/epjconf/20122104004
© Owned by the authors, published by EDP Sciences, 2012

Do light nuclei display a universal γ-ray strength function?

M. Guttormsen[1,a], A.C. Larsen[1], A. Bürger[1], A. Görgen[1], H.T. Nyhus[1], S. Siem[1], N.U.H. Syed[1], H.K. Toft[1], G.M. Tveten[1], S. Harissopulos[2], T. Konstantinopoulos[2], A. Lagoyannis[2], G. Perdikakis[2], A. Spyrou[2], M. Kmiecik[3], K. Mazurek[3], M. Krtička[4], T. Lönnroth[5], M. Norrby[5], A. Schiller[6], and A. Voinov[6]

[1] Department of Physics, University of Oslo, N-0316 Oslo, Norway
[2] Institute of Nuclear Physics, NCSR "Demokritos", Athens, Greece
[3] Institute of Nuclear Physics PAN, Kraków, Poland
[4] Institute of Particle and Nuclear Physics, Charles University, Prague, Czech Republic
[5] Department of Physics, Åbo Akademi University, FIN-20500 Åbo, Finland
[6] Department of Physics and Astronomy, Ohio University, Athens, Ohio 45701, USA

Abstract. In this work we focus on properties in the quasi-continuum of light nuclei. Generally, both level density and γ-ray strength function (γ-SF) differ from nucleus to nucleus. In order to investigate this closer, we have performed particle-γ coincidences using the reactions (p,p'), (p,d) and (p,t) on a ^{46}Ti target. In particular, the very rich data set of the ^{46}Ti$(p,p')^{46}$Ti inelastic scattering reaction allows analysis of the coincidence data for many independent data sets. Using the Oslo method, we find one common level density for all data sets. If transitions to well-separated low-energy levels are included, the deduced γ-SF may change by a factor of $2-3$, due strong to Porter-Thomas fluctuations. However, a universal γ-SF with small fluctuations is found provided that only excitation energies above 3 MeV are taken into account. The nuclear structure of the titaniums is discussed within a combinatorial quasi-particle model, showing that only few Nilsson orbitals participate in building up the level density for these light nuclei.

1 Introduction

The Oslo group has studied the low-energy tail of the giant electric dipole resonance (GEDR) in various mass regions. The method is based on measuring particle-γ coincidences from light-ion reactions with only one charged ejectile. In this way the γ-ray emission can be studied as function of excitation energy up to the particle separation energy. In the framework of the Oslo method, these spectra can be used to simultaneously extract level density and γ-ray strength function (γ-SF).

Many experimental groups have extensively studied the smooth behavior of the GEDR [1]. For heavy nuclei far away from closed shell, the various statistical gross properties vary slowly from nucleus to nucleus, see e.g. [2]. The Oslo group has particularly studied the low-energy tail of the GEDR for rare-earth nuclei. Here, the γ-SF is found to be nicely fitted by the KMF-model [3] with a superimposed Lorentzian originating from the strength of the $M1$-scissors mode[1]. Thus, one may claim that the γ-decay of these nuclei is governed by an underlying γ-SF that is experimentally observable. Figure 1 demonstrates the smooth behavior of the γ-SF in ^{171}Yb.

The level densities are also very similar for neighboring rare earth nuclei, however, there is a pronounced odd-even mass effect. An odd-mass nucleus, say ^{171}Yb, has $5-7$ times more levels than

[a] e-mail: magne.guttormsen@fys.uio.no

[1] Typical resonance parameters of the scissor mode in deformed reare earth nuclei are: $E_\gamma \sim 3$ MeV, $\sigma_{E_\gamma} \sim 1$ MeV and $B(M1) \sim 6\mu_N^2$.

This is an Open Access article distributed under the terms of the Creative Commons Attribution-Noncommercial License 3.0, which permits unrestricted use, distribution, and reproduction in any noncommercial medium, provided the original work is properly cited.

Article available at http://www.epj-conferences.org or http://dx.doi.org/10.1051/epjconf/20122104004

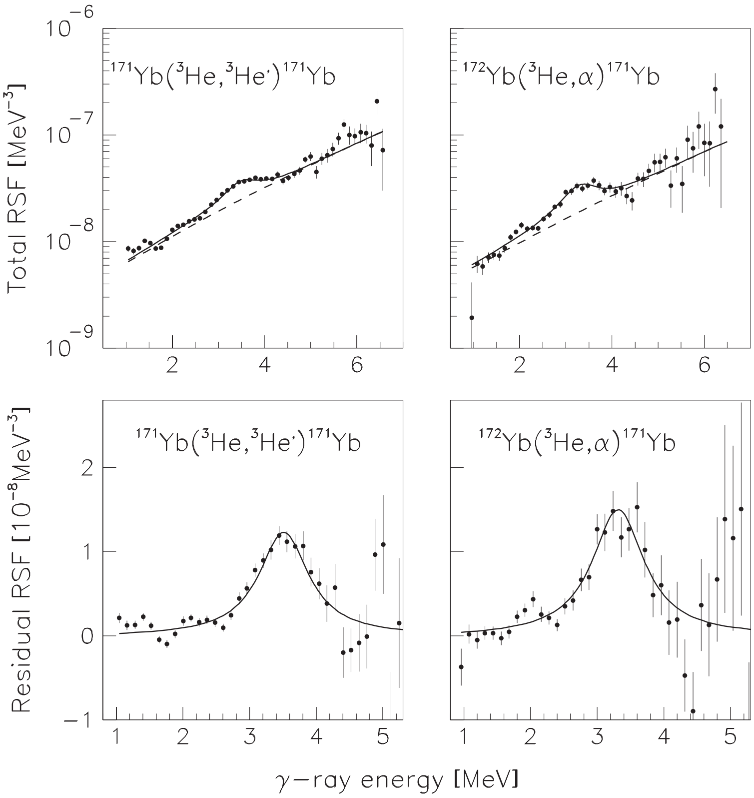

Fig. 1. A pygmy resonance found in ^{171}Yb observed for two different reactions [2]. The solid line in the upper panels is a fit to data including all contributions. The dashed lines are due to the KMF-modeled tail of the GEDR. The difference between the total γ-SF data and the KMF-model is shown in the lower panels.

its even-even neighbors ^{170}Yb and ^{172}Yb. This is due to the fact that nucleons not coupled in Cooper pairs [4], may populate various unoccupied single-particle orbitals and thus contribute significantly to the total level density.

The smooth behavior vanishes for lighter nuclei, typically for nuclei with mass numbers $A < 60$. It may look like each nucleus has its own γ-SF and that the function even depends on excitation energy.

In a recent study [5] the γ decay has been simulated for a light nucleus resembling ^{57}Fe. The level density and γ-SF entering the simulated data are known. It turns out that the Oslo method reproduces the level density, but not the true input γ-SF. The expected γ-decay pattern may be hidden for several reasons related to:

– Low level density
– Irregular spin distribution
– Asymmetric parity distribution

Thus, the nucleus may not have available states with right spin and parity to reveal the fully allowed γ-SF.

In this work we will search for a universal γ-SF in the titanium mass region. In particular the ^{46}Ti$(p, p')^{46}$Ti reaction gives a very rich data set that allows to compare several γ-SFs at different excitation regions.

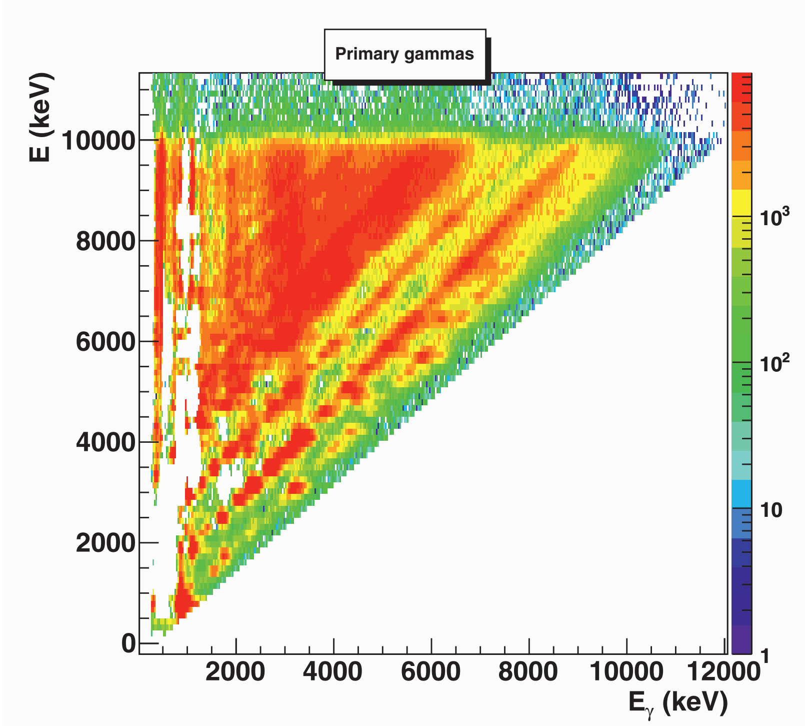

Fig. 2. The first-generation γ-ray matrix of ^{46}Ti obtained from the inelastic proton reaction. Only a part of the $P(E, E_\gamma)$ matrix is utilized, namely data with $E_\gamma > 1.8$ MeV and $5.5 < E < 10$ MeV.

2 Experiments

The experiments were conducted at Oslo Cyclotron Laboratory (OCL) using 15 and 32 MeV proton beams on a self-supporting target of ^{46}Ti. The thickness of the target was 1.8 mg/cm^2. The reactions studied are ^{46}Ti$(p, p')^{46}$Ti, ^{46}Ti$(p, d)^{45}$Ti and ^{46}Ti$(p, t)^{45}$Ti, which have been reported in [6–8]. The charged ejectiles are used to tag the excitation energies for each γ-ray spectrum from the ground state and up to the neutron separation energy.

The particle-γ coincidences are measured with the efficient CACTUS multi-detector array [9]. The coincidence set-up consists of eight collimated ΔE – E type Si particle telescopes, placed at a distance of 5 cm from the target and making an angle of $\theta = 45°$ with the beam line. The particle telescopes are surrounded by 28 5" × 5" NaI γ-ray detectors, which have a total efficiency of ~ 15% of 4π.

The experimental extraction procedure and assumptions made are described in Ref. [10]. The registered ejectil energy is transformed into excitation energy of the residual nucleus through reaction kinematics and the known reaction Q-value. The excited residual nucleus produced in the reaction will subsequently decay by one or several γ-rays. Thus, a γ-ray spectrum can be recorded for each initial excitation energy bin E. Furthermore, the γ-ray spectra are corrected for the NaI detector response function. The unfolding is based on the Compton-subtracting technique [11], which prevents additional count fluctuations to appear in the unfolded spectrum.

The set of these unfolded γ-ray spectra forms the basis for extracting the first-generation γ-ray spectra, which are organized into an (E, E_γ) matrix. Here, the energy distribution of the first (primary) emitted γ-rays in the γ-cascades at various excitation energies are isolated by an iterative subtraction technique [12]. The main assumption of the first-generation method is that the γ-ray spectrum from a bin of excited states are independent of the population mechanism of these states. This means that the γ-spectrum obtained from the direct reaction into states at excitation energy E is similar to the

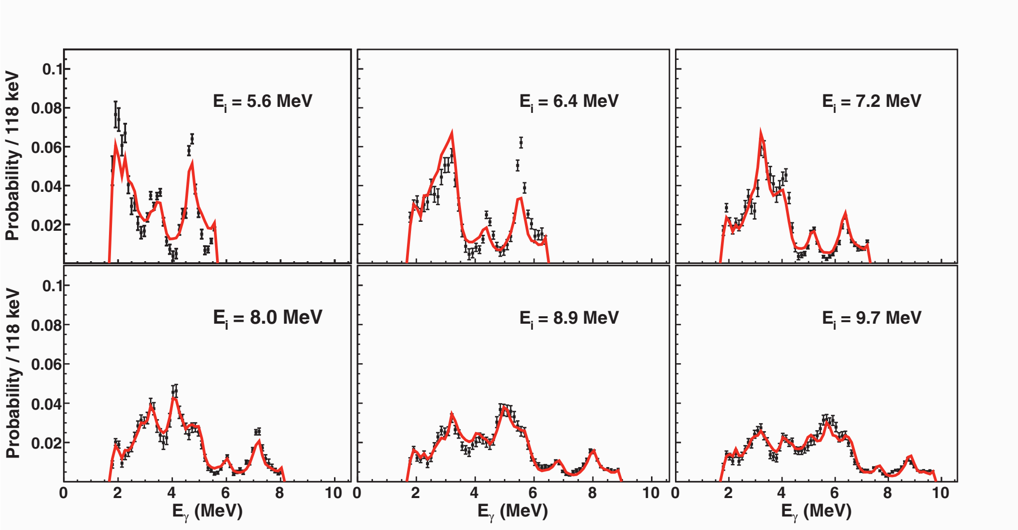

Fig. 3. Comparison between the experimental $P(E_i, E_\gamma)$ matrix (squares) of ^{46}Ti and fitted spectra from one common $\rho(E)$ and $\mathcal{T}(E_\gamma)$ [6].

one obtained if the states at E are populated by γ-decay from higher-lying states. Figure 2 shows the first-generation γ-ray matrix obtained from the ^{46}Ti$(p, p')^{46}$Ti reaction.

3 Level density and γ-SF

The generalized Fermi's golden rule states that the decay probability can be divided into a factor depending on the transition matrix-element between the initial and final state, and the state density at the final states. Following this factorization, we express the decay probability from the initial excitation energy E to depend on the γ-ray transmission coefficient $\mathcal{T}(E_\gamma)$ and the level density $\rho(E - E_\gamma)$ by

$$P(E, E_\gamma) \propto \mathcal{T}(E_\gamma)\rho(E - E_\gamma). \tag{1}$$

Here, $\mathcal{T}(E_\gamma)$ is assumed to be temperature (or excitation energy) independent according to the Brink hypothesis [14].

The ρ and $\mathcal{T}$ functions are determined by an iterative procedure [10] by adjusting these two functions until a global χ^2 minimum with the experimental $P(E, E_\gamma)$ matrix is reached. The quality of the fit is demonstrated in Fig. 3.

It has been shown [10] that if one of the solutions for ρ and $\mathcal{T}$ is known then the entries of the matrix $P(E, E_\gamma)$ in Eq. (1) are invariant under the transformations:

$$\tilde{\rho}(E - E_\gamma) = A \exp[\alpha(E - E_\gamma)]\rho(E - E_\gamma), \tag{2}$$

$$\tilde{\mathcal{T}}(E_\gamma) = B \exp(\alpha\, E_\gamma)\, \mathcal{T}(E_\gamma). \tag{3}$$

The normalization parameters A, B and α are unknown, but can be determined from other experimental data or systematics.

The extracted level density based on data with $E_\gamma > 1.8$ MeV and $5.5 < E_i < 10$ MeV is shown in the left panel of Fig. 4 together with a data point based on Ericson fluctuations [15]. The arrows show the region where the data have been normalized.

The deduced γ-SF for dipole radiation can be calculated from the normalized transmission coefficient $\mathcal{T}(E_\gamma)$ by [16]

$$f(E_\gamma) = \frac{1}{2\pi}\frac{\mathcal{T}(E_\gamma)}{E_\gamma^3}. \tag{4}$$

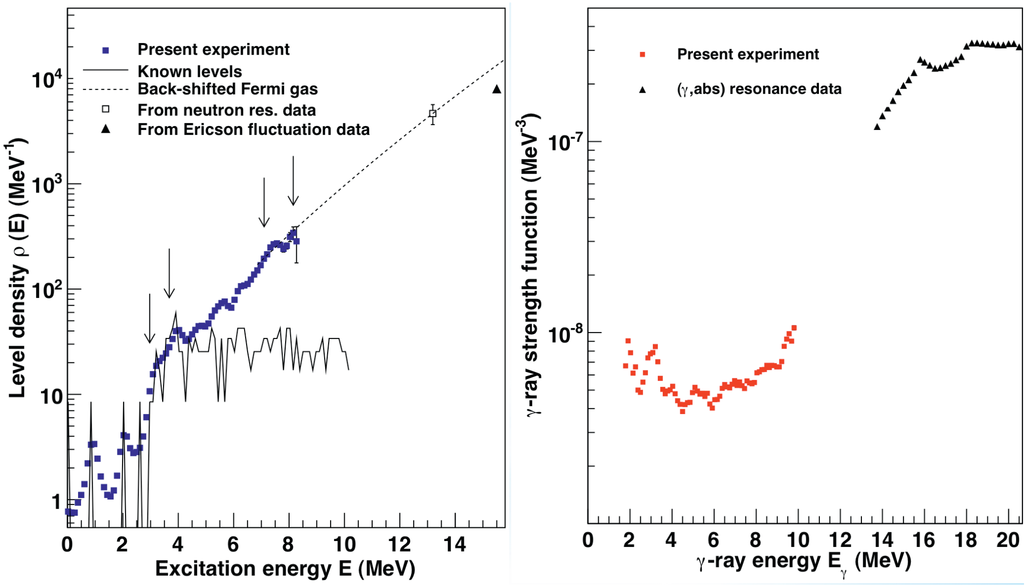

Fig. 4. Left panel: The nuclear level density (filled squares) of ^{46}Ti. At low excitation energies, the data are normalized (between the arrows) to known discrete levels (solid line). At higher excitation energies, the data are normalized to the BSFG level density (dashed line) going through the point $\rho(S_n)$ (open square). For comparison a data point obtained from Ericson fluctuations are shown (black triangle) [15]. Right panel: Experimental γ-SF for ^{46}Ti (squares). For comparison, GEDR data from the (γ, abs) reaction are shown (triangles) [17].

The normalized γ-SF is shown in the right panel of Fig. 4. For comparison, the GEDR data [17] are also shown, which have been translated from photo neutron cross section σ to γ-SF by [16]

$$f(E_\gamma) = \frac{1}{3\pi^2\hbar^2c^2}\frac{\sigma(E_\gamma)}{E_\gamma}. \tag{5}$$

Unfortunately, there is a large energy gap between our data ending at $E_\gamma = 10$ MeV and the GEDR data that start at 14 MeV.

4 Single-particle levels

The ^{44,45,46}Ti isotopes have 2 protons outside the $Z = 20$ shell gap and 2, 3 or 4 neutrons outside the $N = 20$ shell gap, respectively. The ^{40}Ca core is probably not very pronounced since these isotopes have a nuclear quadrupole deformation of $\epsilon \sim 0.3$. Experimentally, this is indicated by a level in ^{45}Ti of $I^\pi = 3/2^+$ from the $\nu d_{3/2}$ single particle hole state appearing at low excitation energy.

The few active particles reveal very different level densities for the three isotopes, as shown in the left panel of Fig. 5. At around 8 MeV of excitation energy, the level densities show only ~ 500 MeV^{-1}. In the ^{170,171,172}Yb isotopes (left panel of Fig. 5) the number of levels is ~ 10.000 times larger. Here, the level densities for the even-even nuclei are almost identical, whereas the odd-mass nucleus has a factor $5-7$ times more levels due to the unpaired valence neutron.

We have used a combinatorial quasi-particle model [7] to study the single-particle Nilsson orbitals involved in building the nuclear level density. The model also gives spin distributions as well as the parity distribution defined by the parity asymmetry parameter:

$$\alpha = \frac{\rho_+ - \rho_-}{\rho_+ + \rho_-}. \tag{6}$$

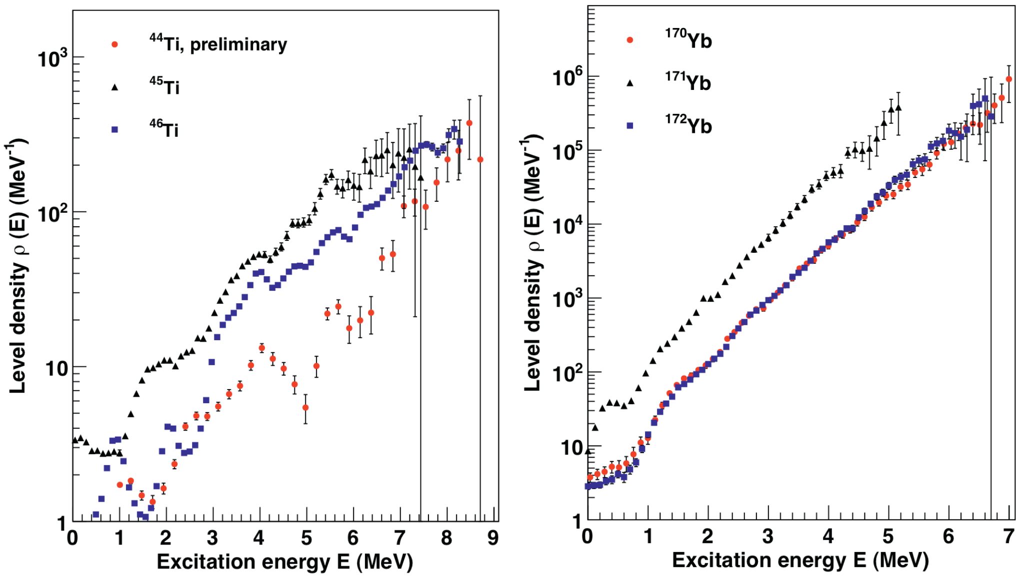

Fig. 5. Comparison between the level densities of ^{44,45,46}Ti and ^{170,171,172}Yb. Typically, rare earth nuclei show parallel level densities (in log scale) and the odd-mass nucleus reveals 5-7 times more levels than its even-even neighbors.

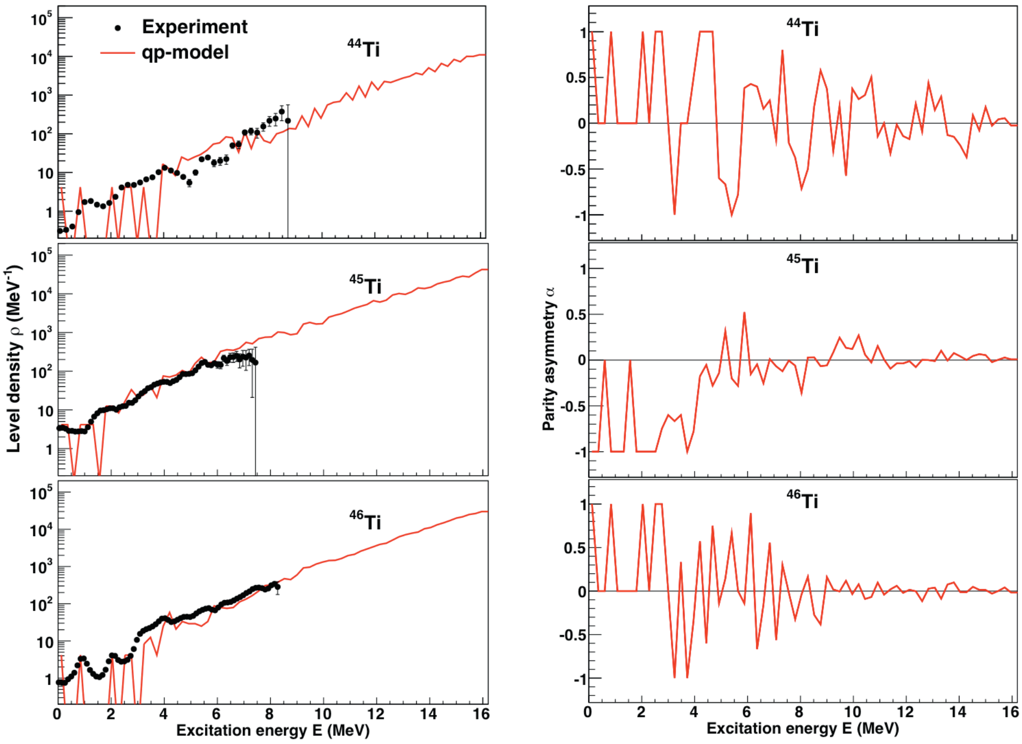

Fig. 6. Model description of level density and parity distribution (red lines). The experimental level densities (black points) are shown for comparison.

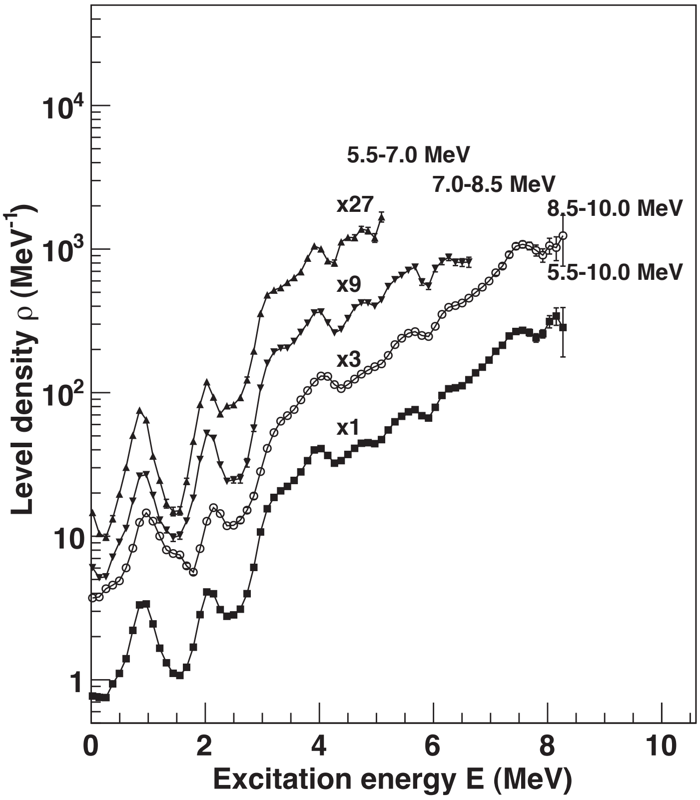

Fig. 7. Level density extracted from statistically independent data sets, taken from various initial excitation energy bins E_i (the three upper curves). The lower curve is the result for the whole energy region of $5.5 < E_i < 10$ MeV.

Figure 6 shows a nice reproduction of the observed level densities in the ^{44,45,46}Ti isotopes. At 8 MeV of excitation energy only about 6 proton and 6 neutron Nilsson orbitals are active. The corresponding number for ytterbiums is more than 30 orbitals of each type. In the later case, there are enough levels with all spins and parities to reveal all types of transitions, and thus the universal γ-SF can be observed.

The level densities seem to increase most strongly around 3 – 4 MeV of excitation energy. Here, the first Cooper pair is probably broken, producing more states. Above 3 – 4 MeV, the parity asymmetry approaches zero on the average. However, below this excitation energy, the parities are predominately positive for the even titaniums, and negative for the odd case, which states the importance of the $f_{7/2}$ orbitals at low excitation energies.

5 The γ-SF at various excitation regions

In the ^{46}Ti$(p, p')^{46}$Ti inelastic scattering reaction more than 110 million events were collected. This high statistics makes it possible to divide the data set of the first-generation matrix (see Fig. 2) into three independent data sets in order to study the γ-SF dependency on excitation energy. The three sets are defined by $5.5 < E_i < 7$ MeV, $7 < E_i < 8.5$ MeV and $8.5 < E_i < 10$ MeV. Figure 7 shows that all level densities are comparable with the global fit of $5.5 < E_i < 10$ MeV. However, the corresponding γ-SFs are not at all equal (not shown). This would indicate that there are no universal γ-SF for this nucleus, but the situation is not that simple.

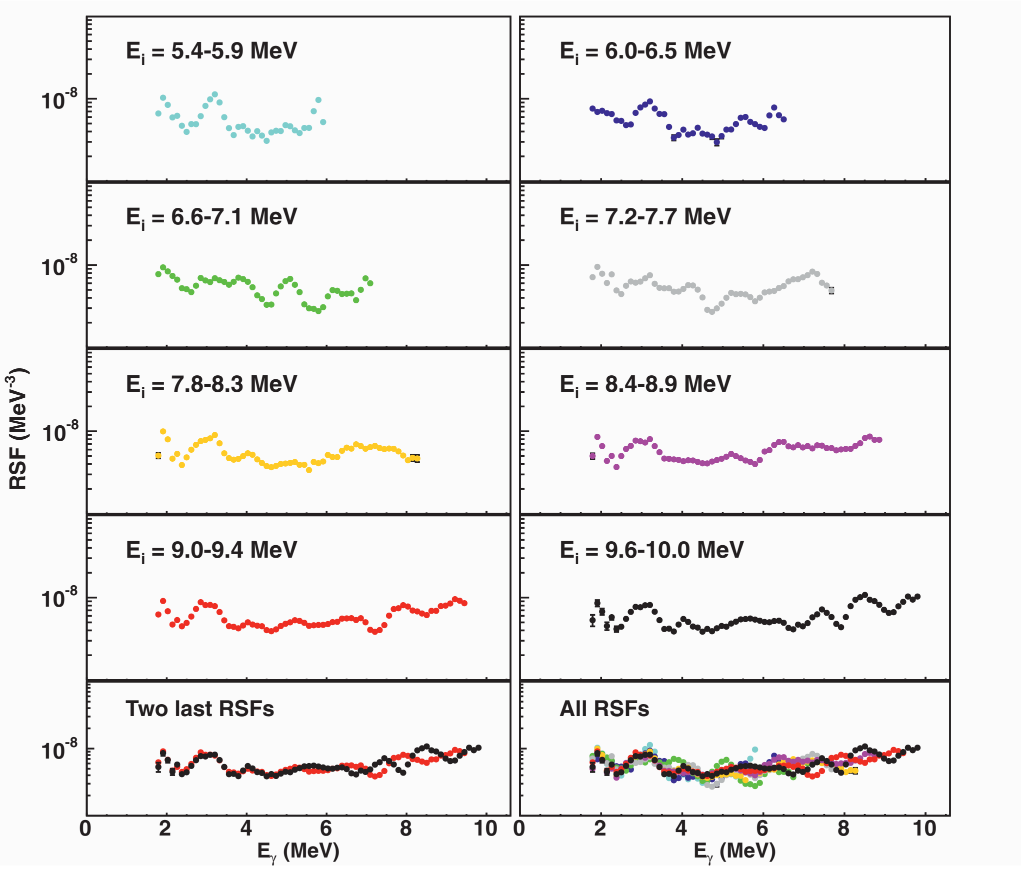

Fig. 8. Deduced γ-SF from various initial excitation bins E_i. The functions are evaluated from the ratio $P(E_i, E_\gamma)/\rho(E_f)$ as described in the text.

In order to study the variations in the γ-SF with excitation energy, we introduce here a new approach [6]. By accepting one common level density, we may investigate the transmission coefficient in detail, and thus the validity of the Brink hypothesis.

We first adopt the solutions $\mathcal{T}$ and ρ from Sec. 3 and rewrite expression (1) as

$$\mathcal{N}(E_i)P(E_i, E_\gamma) \approx \mathcal{T}(E_\gamma)\rho(E_i - E_\gamma). \tag{7}$$

The normalization factor for each initial excitation bin is defined by

$$\mathcal{N}(E_i) = \frac{\int_0^{E_i} \mathrm{d}E_\gamma\, \mathcal{T}(E_\gamma)\rho(E_i - E_\gamma)}{\int_0^{E_i} \mathrm{d}E_\gamma\, P(E_i, E_\gamma)}. \tag{8}$$

Since there exists only one common level density, we construct the counterpart to Eq. (7) in the case that the transmission coefficient depends on the initial excitation energy:

$$\mathcal{N}'(E_i)P(E_i, E_\gamma) \approx \mathcal{T}(E_i, E_\gamma)\rho(E_i - E_\gamma), \tag{9}$$

where $\mathcal{N}'$ is determined analogously to Eq. (8). We expect that $\mathcal{T}(E_i, E_\gamma)$ fluctuates on the average around $\mathcal{T}(E_\gamma)$. Thus, it is reasonable to expect that $\mathcal{N}' \approx \mathcal{N}$, which gives a transmission coefficient of:

$$\mathcal{T}(E_i, E_\gamma) \approx \mathcal{N}(E_i)\frac{P(E_i, E_\gamma)}{\rho(E_i - E_\gamma)} \tag{10}$$

or

$$\mathcal{T}(E_f, E_\gamma) \approx \mathcal{N}(E_f + E_\gamma)\frac{P(E_f + E_\gamma, E_\gamma)}{\rho(E_f)}. \tag{11}$$

In the last expression, the transmission coefficient is given as a function of final excitation energy $E_f = E_i - E_\gamma$.

Roughly speaking, this treatment determines the transmission coefficient by dividing the first-generation matrix by the level density, i.e. $\mathcal{T} = P/\rho$. This, allows in principle to determine $\mathcal{T}$ in small steps of initial or final excitation energies.

Figure 8 shows that the strength functions vary with initial excitation energy. Plotting all γ-SF together in the lower left panel, display a rather chaotic pattern where the functions deviate by of a factor $2-3$. However, if we compare the two last functions, they look similar for γ-energies up to 7 MeV. Thus, it simply looks like levels below $3-4$ MeV of excitation energy introduce the large fluctuations in the γ-strength.

The decay in quasi-continuum can be further investigated. In order to study the γ-SFs obtained from regions of higher level density, we have taken the four highest gates shown in Fig. 8 and only considered data with $E_\gamma < 5.1$ MeV. Thus, these statistically independent γ-SFs are evaluated in quasi-continuum with initial and final excitation energies of roughly $E_i = 8-10$ MeV and $E_f = 3-7$ MeV, respectively. The deduced γ-SFs are presented in the upper panel of Fig. 9. In the lower panel the

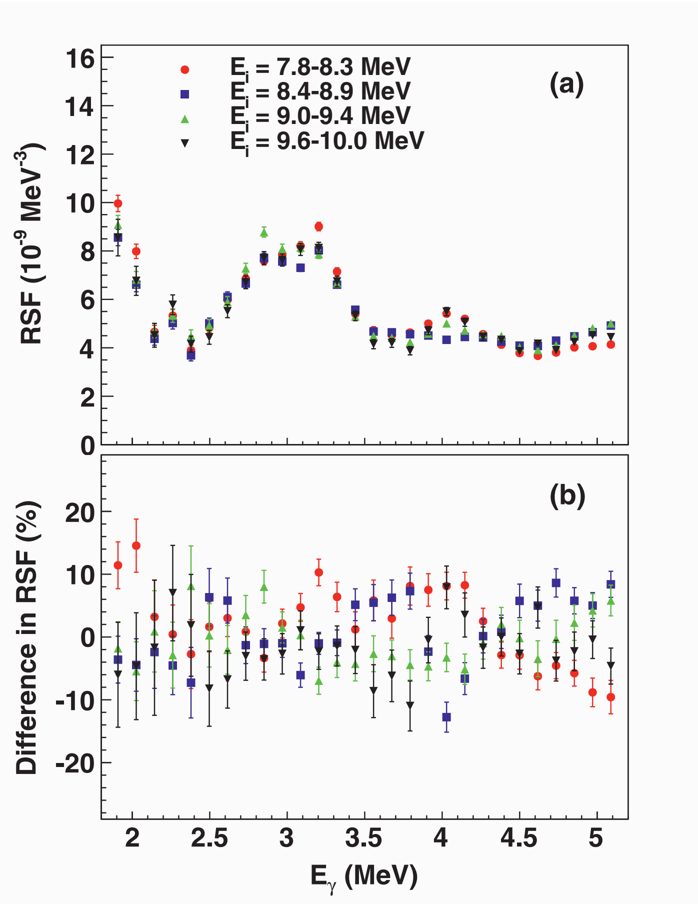

Fig. 9. (a) Gamma-SFs for transitions between states in quasi-continuum. Data from the four highest excitation energy gates of Figs. 8 have been chosen. (b) Ratios of the deviation from the average γ-SF at each γ energy.

relative deviations from the average γ-SF are displayed. Here, we find typical ~ 6 % fluctuations that might be comparable with the Porter-Thomas fluctuations expected in the quasi-continuum of these light nuclei.

6 Summary

The level density and γ-strength function for titaniums have been determined using the Oslo method. Similar level density functions have been extracted from statistically independent data sets covering different excitation energies. This gives confidence to the Oslo method, since the disentanglement of the level density by Fermi's golden rule predicts one and only one unique level density, independent of the data set.

The deduced γ-SF displays an enhancement at low γ-ray energy where we see a bump around 3 MeV and another structure at energies near 2 MeV. A similar enhancement (upbend) has been seen in several other light-mass nuclei and is still not accounted for by present theories.

A method to study the evolution of the γ-SFs as a function of initial and final energy regions has been described. The deduced γ-SFs are found to display strong variations for different initial and final excitation energies if transitions to the lowest excitations are involved. The reason for the violent fluctuations of a factor of $2-3$ is that only a few isolated levels are present at low excitation energies with $E_f < 3$ MeV. The differences in the γ-SFs obtained from a few number of transitions, that can be explained as a consequence of Porter-Thomas fluctuations of individual intensities, show that this energy region cannot be used for determination of the universal γ-SF.

However, the present work shows that it is possible to get more precise experimental information on the universal γ-SF. By imposing restrictions on the initial and final excitation energies, the γ-SFs for the decay between states in quasi-continuum can be extracted (i.e. for $E_f \gtrsim 3$ MeV). The results from this selected data set show that the decay is consistent with a γ-SF which is independent of excitation energy within less than ~ 6 % already at these relatively low excitations. Thus, provided that we use data from the quasi-continuum, a universal γ-SF in the light mass region of the ^{46}Ti nucleus can be extracted.

References

1. S.S. Dietrich and B.L. Berman, At. Data Nucl. Data Tables **38**, 199 (1988).
2. U. Agvaaluvsan, A. Schiller, J.A. Becker, L.A. Bernstein, P.E. Garrett, M. Guttormsen, G.E. Mitchell, J. Rekstad, S. Siem, A. Voinov, and W.Younes, Phys. Rev. C **70**, 054611 (2004).
3. S.G. Kadmenskii, V.P. Markushev, and V.I. Furman, Yad. Fiz. **37** , 227 (1983).
4. J. Bardeen, L.N. Cooper, and J.R. Schrieffer, Phys. Rev. **108**, 1175 (1957).
5. A.C. Larsen, M. Guttormsen, M. Krtička, E. Běták, A. Bürger, A. Görgen, H.T. Nyhus, J. Rekstad, A. Schiller, S. Siem, H.K. Toft, G.M. Tveten, A. Voinov and K. Wikan, Phys. Rev. C **83**, 034315 (2011).
6. M. Guttormsen, A.C. Larsen, A. Bürger, A. Görgen, S. Harissopulos, M. Kmiecik, T. Konstantinopoulos, M. Krtička, A. Lagoyannis, T. Lönnroth, K. Mazurek, M. Norrby, H.T. Nyhus, G. Perdikakis, A. Schiller, S. Siem, and A. Spyrou, N.U.H. Syed, H.K. Toft, G.M. Tveten, and A. Voinov, Phys. Rev. C **83**, 014312 (2011).
7. N.U.H. Syed, A.C. Larsen, A. Bürger, M. Guttormsen, S. Harissopulos, M. Kmiecik, T. Konstantinopoulos, M. Krtička, A. Lagoyannis, T. Lönnroth, K. Mazurek, M. Norrby, H.T. Nyhus, G. Perdikakis, S. Siem, and A. Spyrou, Phys. Rev. C **80**, 044309 (2009).
8. A.C. Larsen, S. Goriely, A. Bürger, M. Guttormsen, A. Görgen, S. Harissopulos, M. Kmiecik, T. Konstantinopoulos, M. Krtička, A. Lagoyannis, T. Lönnroth, K. Mazurek, M. Norrby, H. T. Nyhus, G. Perdikakis, A. Schiller, S. Siem, and A. Spyrou, N.U.H. Syed, H.K. Toft, G.M. Tveten, and A. Voinov Phys. Rev. C, (2011), to be published.
9. M. Guttormsen, A. Atac, G. Løvhøiden, S. Messelt, T. Ramsøy, J. Rekstad, T.F. Thorsteinsen, T.S. Tveter, and Z. Zelazny, Phys. Scr. **T 32**, 54 (1990).

10. A. Schiller, L. Bergholt, M. Guttormsen, E. Melby, J. Rekstad, and S. Siem, Nucl. Instrum. Methods Phys. Res. A **447**, 498 (2000).
11. M. Guttormsen, T.S. Tveter, L. Bergholt, F. Ingebretsen, and J. Rekstad, Nucl. Instrum. Methods Phys. Res. A **374**, 371 (1996).
12. M. Guttormsen, T. Ramsøy, and J. Rekstad, Nucl. Instrum. Methods Phys. Res. A **255**, 518 (1987).
13. Data extracted using the NNDC On-Line Data Service from the ENSDF database.
14. D.M. Brink, Ph.D. thesis, Oxford University, 1955.
15. Merico Salas-Bacci, Steven M. Grimes, Thomas N. Massey, Yannis Parpottas, Raymond T. Wheller, and James E. Oldendick, Phys. Rev. C **70**, 024311 (2004).
16. RIPL-3 Handbook for calculation of nuclear reaction, (2009); available at *http://www-nds.iaea.org/RIPL-3/*
17. B.S. Ishkhanov, I.M. Kapitonov, E.I. Lileeva, E.V. Shirokov, V.A. Erokhova, M.A. Elkin, A.V. Izotova, Moscow State Univ. Inst. of Nucl. Phys., Reports No.2002, p.27/711 (2002).